Simulations of a 3D-segmented Asymmetric Body Coil for Parallel Transmission

I. Graesslin[1], S. Biederer[1], K. Falaggis[1], D. Glaesel[1], P. Vernickel[1], U. Katscher[1], and P. Börnert[1]
[1]Philips Research Europe, Hamburg, Germany

Introduction

Three-dimensional RF excitation pulses [1] are of high interest for applications such as improved slice selective excitation, zoom imaging or spin labeling in perfusion imaging. However, the duration of 3D RF pulses is limited by the finite lifetime of the transverse magnetization and the main field homogeneity. This drawback can be overcome by accelerating the 3D RF pulses via parallel transmission [2-4]. To fully exploit the potential of parallel transmission, RF coil arrays are needed, which allow pulse acceleration in all three spatial directions. 3D-segmented coil arrays can enhance the performance and quality of accelerated 3D RF pulses. This paper discusses simulations of 3D Transmit SENSE pulses using a 24-channel body coil with three consecutive rings, each consisting of eight cylindrically arranged transmit elements. 3D-acceleration is superior with respect to pattern reproduction and RF power requirements.

Methods

The RF coil sensitivities of an asymmetric 24-channel body coil (eight cylindrically arranged elements, segmented two times in z-direction) were simulated (Fig. 1). For the calculation, ideally decoupled TEM transmit resonators were assumed. The model is based on the eight-channel design presented in [5]. The coil was simulated using the finite-difference time-domain (FDTD) method ("XFDTD", Remcom, Inc., USA). The coil sensitivities were calculated on a 5mm grid using various numerical phantoms, as e.g. a cylinder of 140mm in diameter and 50mm in length. The phantoms were placed in the coil centered in z-direction. Various offset positions in x- and y-direction (up to 70mm) were simulated. Furthermore, the dimension of the cylinder in x-direction was varied to mimic an object approximately resembling the coarse body shape. Finally, the bio-mesh model (courtesy PMS Cleveland) of the "Visible Human Male" [6] was used for comparison. Different three-dimensional excitation patterns were applied that were centered in the field-of-excitation (FOX), e.g. a 3D sphere with a diameter of 50% of the FOX, a 3D checkerboard, and a cube. Different matrix sizes N for the FOX discretization were used up to a resolution of N=16×16×16 pixels. Various eight-element coil configurations were simulated: (a) one ring of eight elements, (b) the four even elements in ring one and the odd elements in ring two ("rotated coil"), (c) only the even elements in both rings ("non-rotated coil"). Furthermore, 16 and 24 elements were used in analogous configurations.

The 3D RF pulse calculation for parallel transmission was carried out using an extended version of the 2D RF excitation pulse algorithm described in [7]. The algorithm was implemented in analogy with the non-Cartesian SENSE reconstruction [8]. For the calculation of the RF excitation pulse, the direct matrix inversion was replaced by the more efficient iterative conjugate-gradient method. For the 3D RF-pulses, a stack of spiral trajectories and acceleration factors up to R=16 were applied.

Results and Discussion

For the non-rotated coil, the resulting pulse energy is higher than for the rotated coil for all reduction factors and all demand patterns investigated. Fig. 2 shows the result for the 3D checkerboard pattern. The result can be motivated by the complementary sensitivity distributions of the two mutually rotated rings. For a reduction factor R=1(4), the pulse energy of the rotated coil is a factor of 0.65 (0.78) lower than for the non-rotated coil (see Fig. 3). The pulse energy increases roughly quadratically with the reduction factor as predicted in previous studies [9].

$R_{in-plane}$	$R_{throug-plane}$	R_{total}	Norm. pulse energy
1.0	1.0	1.0	1.0
2.7	1.0	2.7	24.1
1.6	1.6	2.6	17.1
4.0	1.0	4.0	57.7
2.0	2.0	4.0	41.3

Tab. 1: Dependency of normalized pulse energy on different reduction factors R.

Tab. 1 shows the pulse energy for different reduction factors using a spherical excitation pattern on a 16×16×16 grid. The data are normalized to the corresponding non-accelerated case (16 spirals, 8 revolutions each). A total reduction factor R_{tot} = 4 can be realized in 2D via 16 spirals with 2 revolutions each ($R_{in-plane}$ = 4, $R_{through-plane}$ = 1), or in 3D via 8 spirals with 4 revolutions each ($R_{in-plane}$ = 2, $R_{through-plane}$ = 2). The 3D case results in a 30% reduction of the pulse energy. The same result is found for the case R_{tot} = 3 (see Tab. 1). This finding corresponds to the analogous behavior in parallel imaging [10].

The iterative calculation of multi-dimensional RF excitation pulses for Transmit SENSE is advantageous compared with the direct matrix inversion, in particular for larger matrix sizes with respect to the calculation time [11].

Conclusion

3D-segmented coil geometries, e.g., the z-segmented body coil, but also planar and flexible transmit coil arrays will make 3D pulses practical in the future. Furthermore, these types of coils allow an acceleration of Transmit SENSE in arbitrary spatial directions, e.g. oblique or double oblique slices or volumes. The presented simulations show, that the coil geometry has a significant impact on the pulse energy. It is expected that these findings will also be applicable for the global and local SAR.

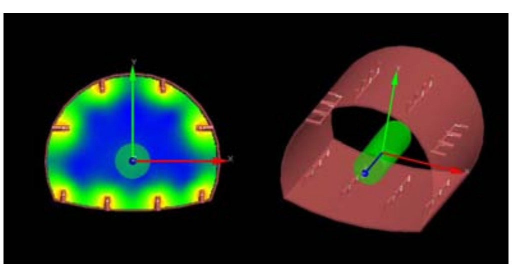

Fig. 1: Spatial B_1-field distribution of the front view of a 24-element asymmetric body coil (twice z-segmented) with a centered cylinder (a). 3D view of the coil (b).

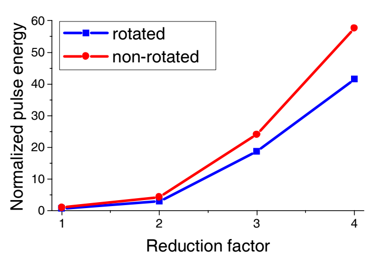

Fig. 2: Normalized pulse energy of rotated coil elements and non-rotated coils.

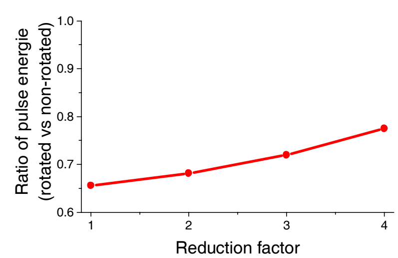

Fig. 3: Ratio of pulse Energy of rotated coils vs. non-rotated coils.

References

[1] Pauly J, et al. [1989] MRM 81:43-56
[2] Katscher U, et al. [2003] MRM 49:144-150
[3] Zhu Y [2004] MRM 51:775-784
[4] Grissom W, et al. [2005] ISMRM 13:19
[5] Luedeke KM, et al. [2003] ISMRM 11:2352
[6] "Visible Human Project" NLM [1996]
[7] Graesslin I, et al. [2005] MAGMA 18:S109
[8] Pruessmann KP, et al. [2001] MRM 46:638-651
[9] Katscher U, et al. [2005] ISMRM 13:17
[10] Weiger M et al. [2002] MAGMA 14:10-19
[11] Graesslin I, et al. [2006] ISMRM 14:2470